ARTICLE NO. 80-0325R

# Studies of Leading-Edge Thrust Phenomena

Harry W. Carlson* and Robert J. Mack*
*NASA Langley Research Center, Hampton, Va.*

**A study of practical limitations on achievement of theoretical leading-edge thrust has been made and an empirical method for estimation of attainable thrust has been developed. The method is based on 1) a theoretical analysis of a set of two-dimensional airfoils to define thrust dependence on airfoil geometric characteristics and arbitrarily defined limiting pressures, 2) an examination of two-dimensional airfoil experimental data to provide an estimate of limiting pressure dependence on local Mach number and Reynolds number, and 3) employment of simple sweep theory to adapt the method to three-dimensional wings. Because the method takes into account the spanwise variation of airfoil section characteristics, an opportunity is afforded for design by iteration to maximize the attainable thrust and the attendant performance benefits. The applicability of the method was demonstrated by comparisons of theoretical and experimental aerodynamic characteristics for a series of wing-body configurations. Generally, good predictions of the attainable thrust and its influence on lift and drag characteristics were obtained over a range of Mach numbers from 0.24 to 2.0.**

## Nomenclature

$b$ = wing span
$c$ = local wing chord
$\bar{c}$ = mean aerodynamic chord
$c_{av}$ = average wing chord, $S/b$
$c_{p,\lim}$ = limiting pressure coefficient used in definition of attainable thrust
$c_{p,\text{vac}}$ = vacuum pressure coefficient, $-2/\gamma M^2$
$c_t$ = theoretical thrust coefficient, $dt/dy\, qc$
$c_t^*$ = attainable section thrust coefficient, $dt^*/dy\, qc$
$c_v$ = vortex force coefficient, $(c_t - c_t^*)\cos\Lambda_{le}$
$C_A$ = axial or chord force coefficient
$C_D$ = drag coefficient
$C_L$ = lift coefficient
$C_p$ = pressure coefficient
$C_T$ = theoretical wing thrust coefficient,

$$\frac{2}{b}\int_0^{b/2} c_t\left(\frac{c}{c_{av}}\right)dy$$

$C_T^*$ = attainable wing thrust coefficient,

$$\frac{2}{b}\int_0^{b/2} c_t^*\left(\frac{c}{c_{av}}\right)dy$$

$k_1,k_2,k_3,k_4$ = constants used in airfoil section definition
$K_T$ = fraction of theoretical thrust actually attainable $c_t^*/c_t$
$M$ = Mach number
$M_\infty$ = freestream Mach number
$M_e$ = equivalent Mach number used in definition of $K_T$
$q$ = dynamic pressure
$r$ = leading-edge radius
$R$ = freestream Reynolds number based on $\bar{c}$
$S$ = wing area
$t$ = theoretical section leading-edge thrust
$t^*$ = attainable section leading-edge thrust
$x,y,z$ = Cartesian coordinate system
$\alpha$ = angle of attack, rad (unless otherwise specified)
$\gamma$ = ratio of specific heats
$\eta$ = location of maximum wing section thickness as fraction of chord
$\Lambda_{le}$ = leading-edge sweep angle, deg
$\Lambda_{te}$ = trailing-edge sweep angle, deg
$\Lambda_v$ = vortex action line sweep angle, deg
$\tau$ = maximum wing section thickness

*Subscripts*

$k$ = 1,2,3,4
$n$ = quantities pertaining to wing section normal to leading edge with maximum thickness at midchord (Fig. 10)

Received Jan. 10, 1980; presented as Paper 80-0325 at the AIAA 18th Aerospace Sciences Meeting, Pasadena, Calif., Jan. 14-16, 1980, revision received March 31, 1980. This paper is declared a work of the U.S. Government and therefore is in the public domain.

Index categories: Aerodynamics; Computational Methods.

*Aero-Space Technologist, Supersonic Aerodynamics Branch, High-Speed Aerodynamics Division. Member AIAA.

## I. Introduction

LEADING-EDGE thrust is an important but little understood aerodynamic phenomenon that can have a large influence on wing aerodynamic performance. This force results from the high local velocities and the accompanying low pressures which occur as air flows from a stagnation point on the undersurface of the wing around the leading edge to the upper surface. At low subsonic speeds, the high aerodynamic efficiency of uncambered wings with high aspect ratios depends directly on the presence of leading-edge thrust to counteract the drag arising from pressure forces acting on the remainder of the airfoil. Leading-edge thrust tends to diminish with increasing speeds, but may be present to some degree even in the supersonic speed regime, provided the leading edge is rounded and swept behind the Mach angle.

Leading-edge thrust for subsonic speeds may be predicted by a variety of methods including a vortex-lattice program[1] capable of handling wings of complex planform. At supersonic speeds, leading-edge thrust for flat wings with straight leading edges may be determined by purely analytic means (e.g., Ref. 2). A recently developed computer method[3] has extended this capability to wings of arbitrary planform with twist and camber. These methods, however, provide estimates of only the theoretical thrust which may or may not be attainable in the real flow.

This paper reviews a recently completed study of the factors limiting thrust development and describes an empirical method for the estimation of attainable thrust, which may be programmed as a subroutine in existing lifting surface

computer programs. The underlying analysis on which the prediction method depends, originally presented in Ref. 4, is herein redescribed in what is believed to be a more easily understandable form. The present paper also presents an improved system for application of the method to flat or twisted and cambered wings at supersonic speeds. The applicability of the method is demonstrated by comparisons of theoretical and experimental aerodynamic characteristics for a series of wing-body configurations.

## II. Review of Attainable Thrust Study

Development of this method for the prediction of attainable leading-edge thrust is based on the fundamental principle that such forces result from pressures acting on a surface, and limitations on the attainable pressures and the surface areas on which they act form the only restraints on the achievement of theoretical thrust. As illustrated in Fig. 1, the study may be considered to cover three distinct phases. First, a program for two-dimensional subsonic airfoils was employed to define limitations on the theoretical thrust imposed by airfoil geometry restraints and by arbitrarily defined limiting pressures. Then, experimental data for two-dimensional airfoils were used to evaluate practical limiting pressures and their dependence on Mach number and Reynolds number. Finally, to extend the applicability of the analysis to three-dimensional wings, simple sweep theory was used to establish the relationships between streamwise airfoil sections and sections normal to the leading edge.

## III. Theoretical Two-Dimensional Airfoil Analysis

A typical pressure distribution for a symmetrical airfoil section at a moderate angle of attack is illustrated in Fig. 2. Pressures are plotted as a function of distance along the chord line and also as a function of distance normal to the chord line. Integration of the pressure curve in the first plot yields the section normal force; integration of the curve in the second yields the section thrust coefficient. An important feature of this pressure distribution is the large suction pressure peak in the vicinity of the nose of the airfoil. This is, in fact, the dominant feature of the second plot and thus is the dominant factor in the determination of the section thrust coefficient. Linearized theory places no bounds on the magnitude of the peak suction pressure, which, therefore, can become much greater than practically realizable values. In particular, the theory can easily call for pressures which exceed the vacuum limit depicted on the figure. As can be seen here, limitations imposed by practically realizable pressures may have a relatively insignificant effect on the normal force but could, at the same time, severely limit the attainment of the thrust force.

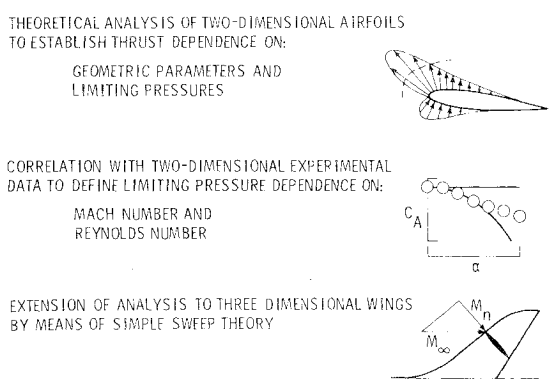


**Fig. 1 Major elements of the attainable thrust study.**

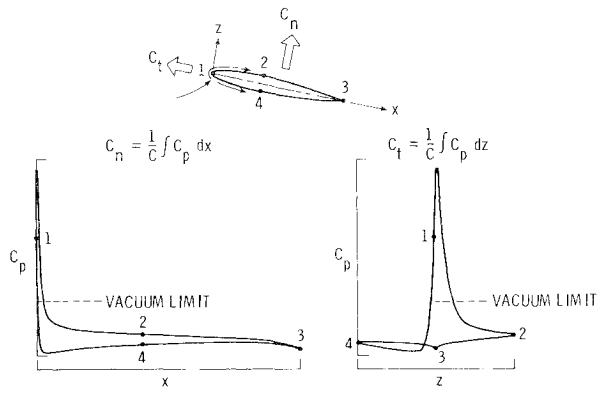


**Fig. 2 Typical theoretical pressure distribution.**

For the series of symmetrical two-dimensional airfoil sections shown in Fig. 3, the subsonic airfoil program of Ref. 5 was employed to define pressure distributions and integrated thrust coefficients. The airfoils were defined by the following equation:

$$z = k_1\sqrt{x} + k_2 x + k_3 x^{3/2} + k_4 x^2$$

in which the coefficients were selected to produce the required chord, thickness, and leading-edge radius for a wing section with maximum thickness at midchord. Maximum airfoil thickness ranged from 6 to 18% of the chord, and leading-edge radius ranged from 2 to 16% of the maximum thickness. For a given airfoil, pressure distributions and coefficients covering a range of Mach numbers were found by applying the Prandtl-Glauert rule,

$$C_p\sqrt{1-M_n^2} = \text{const}$$

to pressure distributions obtained at a Mach number of 0.01. This simple means of handling Mach number effects was employed for the sake of consistency with methods using linearized theory for estimating theoretical thrust. Program values of the integrated section thrust coefficient

$$c_t = \frac{1}{c}\int C_p\,dz$$

were found to be relatively independent of the airfoil thickness and the leading-edge radius and to be in reasonably good agreement with the two-dimensional theoretical value.

In order to determine the effect on the thrust coefficient of more realistically attainable pressure distributions, the program integration was performed twice—once without limitation and once with limitation to values greater than or equal to the vacuum pressure coefficient (limiting the suction peak). Definition of effective limiting pressures more restrictive than the vacuum limit will be discussed in a later section of the paper. This limitation is intended to account, in an approximate way, for two of the factors which limit at-

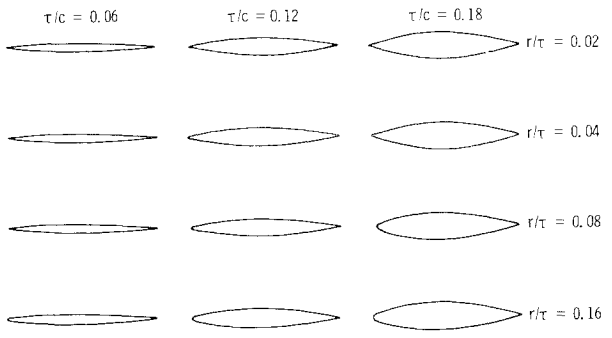


**Fig. 3 Airfoil sections employed in study.**

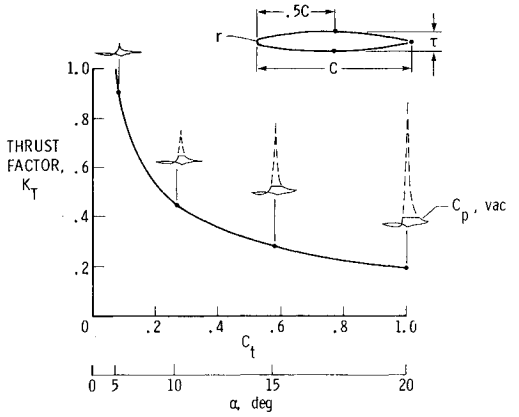


**Fig. 4 Typical program evaluation of the thrust factor for a vacuum pressure limitation.**

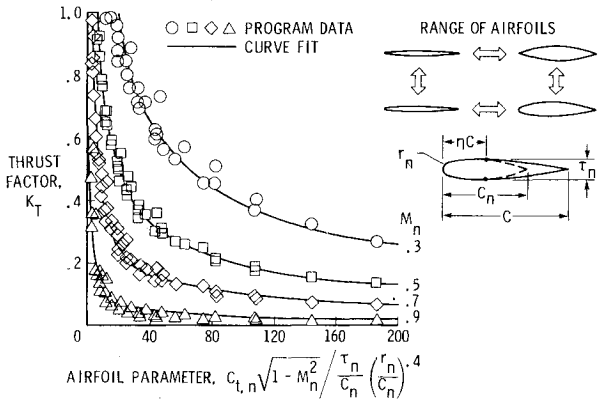


**Fig. 5 Thrust factor dependence on airfoil parameters for a vacuum pressure limitation.**

tainable thrust: the failure to attain theoretical peak suction pressures and the tendency of these peaks to occur at a more rearward position on the airfoil. The limited value of $c_t$ is designated $c_t^*$ and the attainable thrust ratio or the thrust factor is simply: $K_T = c_t^*/c_t$.

Shown in Fig. 4 is an example of the variation of the thrust factor with angle of attack (and with the theoretical thrust coefficient) for a given airfoil section at a given Mach number. Inset sketches show pressure distributions for 5,10,15, and 20 deg angles of attack. As the figure shows, the vacuum pressure limitation can be quite severe for large angles.

Program data are shown in Fig. 5 for the complete range of airfoil parameters and for Mach numbers of 0.3, 0.5, 0.7, and 0.9. For a given Mach number, the thrust factor $K_T$ was found to correlate well with the parameter

$$c_{t,n}\sqrt{1-M_n^2}/(\tau_n/c_n)(r_n/c_n)^{0.4}$$

The subscript $\eta$ refers to quantities associated with an airfoil section with maximum thickness at midchord. For a two-dimensional airfoil with an arbitrary location of maximum thickness $\eta$: $c_n = 2\eta c$, $\tau_n = \tau$, $r_n = r$ $M_n = M_\infty$, and $c_{t,n} = c_t(c/c_n)/2\eta$. This substitution permits the program-generated data for sections with maximum thickness at the midchord to be applicable to a wider variety of shapes. It is based on the premise that thrust characteristics are determined almost entirely by the nose section geometry and are little affected by geometry changes aft of the maximum thickness. In the section of the paper dealing with the extension of the analysis to three-dimensional wings, a broader interpretation is given to the use of the subscript $n$. In general,

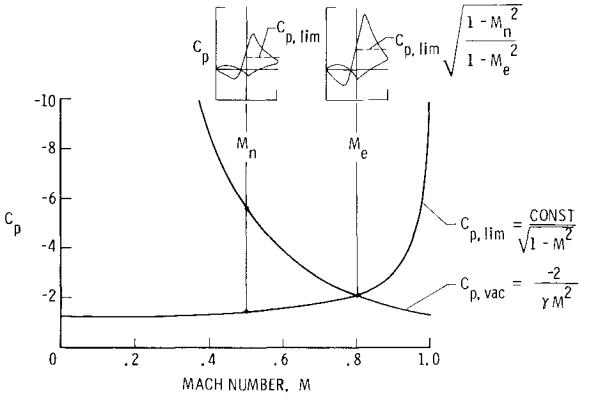


**Fig. 6 Determination of an effective Mach number for an arbitrary pressure limitation.**

it designates properties of a section normal to the leading edge of a swept leading-edge wing with maximum thickness at the midchord.

In Fig. 5, a thrust factor which decreases with increasing theoretical thrust is clearly shown. The correlation plot also shows the tendency of increased thickness or increased leading-edge radius to improve the thrust factor. The curve fit is described by a single equation covering the full range of airfoil parameters and Mach numbers.

$$K_T = \frac{2(1-M_n^2)}{M_n}\left[\frac{\frac{\tau_n}{c_n}\left(\frac{r_n}{c_n}\right)^{0.4}}{c_{t,n}\sqrt{1-M_n^2}}\right]^{0.6} \quad \text{but not greater than 1.0} \tag{1}$$

The limitation of $K_T$ to values no greater than 1.0 permits attainable thrust to equal but not exceed the theoretical thrust. Note that the curve fit allows the thrust to go to zero when either the thickness or the leading-edge radius goes to zero. If both thickness and leading-edge radius go to zero, zero thrust is to be expected. However, as long as there is some thickness, an airfoil with a leading-edge radius of zero could produce a small amount of thrust because of the upper-surface suction pressure peak acting on forward facing slopes. Probably a more important consideration is that real leading-edge radii can never be zero and some attempt should be made to estimate an effective leading-edge radius with theoretically sharp edges.

Equation (1) was developed to cover data in which the limiting pressure coefficient was set equal to the vacuum pressure coefficient. The results, however, can be generalized to cover a full range of limiting pressures between 0 and $C_{p,\text{vac}}$ for a given Mach number $M_n$ by means of the following logic. As illustrated by the pressure distributions shown in Fig. 6, for a given airfoil section at a given angle of attack, the pressure coefficient at any point on the airfoil will vary with Mach number according to the Prandtl-Glauert rule. If the limiting pressure $C_{p,\lim}$ changes in this same fashion, the thrust factor $K_T$ will be the same at all Mach numbers. Thus, for any Mach number $M_e$ different from the Mach number under consideration, $K_T$ will be the same as for $M_n$ provided that

$$C_{p,\lim}(M_e) = C_{p,\lim}(M_n)\frac{\sqrt{1-M_n^2}}{\sqrt{1-M_e^2}}$$

If $M_e$ is selected so that $C_{p,\lim}(M_e)$ is equal to the limiting vacuum pressure for that Mach number $C_{p,\text{vac}}(M_e)$, the appropriate value of $K_T$ for the Mach number under consideration can be found from Eq. (1) by substituting $M_e$ for $M_n$. The required $M_e$ can be found by setting $C_{p,\text{vac}}(M_e)$

equal to $C_{p,\lim}(M_e)$ and solving for $M_e$. Thus,

$$C_{p,\text{vac}}(M_e) = C_{p,\lim}(M_e)$$

or

$$\frac{-2}{\gamma M_e^2} = C_{p,\lim}(M_n)\frac{\sqrt{1-M_n^2}}{\sqrt{1-M_e^2}}$$

and, on solving for the equivalent Mach number,

$$M_e = \frac{-\sqrt{2}}{\gamma C_{p,\lim}\sqrt{1-M_n^2}}\left[\sqrt{1+(\gamma C_{p,\lim}\sqrt{1-M_n^2})^2}-1\right]^{1/2} \quad (2)$$

Thus, the thrust factor can be expressed as

$$K_T = \frac{2(1-M_e^2)}{M_e}\left[\frac{\frac{\tau_n}{c_n}\left(\frac{r_n}{c_n}\right)^{0.4}}{c_{t,n}\sqrt{1-M_n^2}}\right]^{0.6} \text{ but not greater than } 1.0 \quad (3)$$

where $M_e$, as defined by Eq. (2), covers the full range of possible limiting pressures. These expressions [Eqs. (2) and (3)] describe the variation of the thrust factor with the theoretical thrust, with airfoil parameters, with Mach number, and with limiting pressure coefficients, which will be defined in the next section. Figure 7 depicts the final form of thrust factor dependence on airfoil parameters and on an arbitrarily defined limiting pressure coefficient.

## IV. Experimental Two-Dimensional Airfoil Analysis

In order to define practical values of the limiting pressure coefficient, the as yet incomplete prediction method was applied to experimental two-dimensional airfoil data[6,7] for symmetrical sections. As illustrated in Fig. 8, correlations of axial force coefficients calculated by this method with experimentally determined axial force coefficient were used to determine, by iteration, values of $C_{p,\lim}$ which appeared to match the experimental trends. There is clearly a trend of reduced leading-edge thrust coefficients and reduced limiting pressure coefficients required for correlation as the Mach number increases. A more complete set of data used in the definition of limiting pressure coefficient is given in Ref. 4. This study revealed a need for better and more complete two-dimensional airfoil data for symmetrical sections. In particular, a greater range of angle of attack and a greater range of Reynolds number would be desirable.

A summary of the data used in defining the limiting pressure coefficient is shown in Fig. 9. The ratio of the limiting pressure to the vacuum pressure is shown as a function of the Mach number. There is obviously a strong dependence of the limiting pressure coefficient ratio on the Mach number. Although the absolute value of the pressure coefficient decreases with increasing Mach number, the fraction of the vacuum pressure increases to values approaching 1.0 for Mach numbers near 1.0. There is also a weak but definite tendency of the limiting pressure coefficient to increase with increasing Reynolds number. The curve fit shown on Fig. 9 is intended to cover the Mach number and Reynolds number trends of the data. The curve fit is defined by the equation:

$$C_{p,\lim} = \frac{-2}{\gamma M_n^2}\left[\frac{R_n \times 10^{-6}}{R_n \times 10^{-6} + 10^{(4-3M_n)}}\right]^{0.05+0.35(1-M_n)^2} \quad (4)$$

This form was chosen to allow the limiting pressure to approach the vacuum pressure as the Reynolds number approached infinity and to allow the limiting pressure to approach zero as the Reynolds number approached zero. With the definition of effective limiting pressure coefficients, the two-dimensional analysis portion of the study is now complete.

## V. Extension of Analysis to Three-Dimensional Wings

In order to develop an attainable thrust prediction method applicable to three-dimensional wings, the familiar concepts of simple sweep theory were employed. As shown in Fig. 10, the freestream flow is separated into two parts, with one component of velocity parallel to the leading edge and the other perpendicular or normal to the leading edge. It is

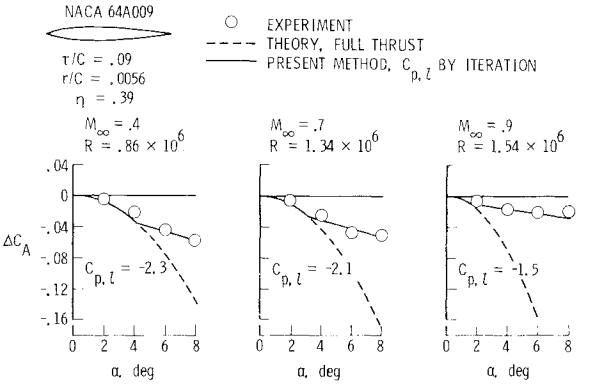


**Fig. 8 Sample of data used in the evaluation of a limiting pressure coefficient.**

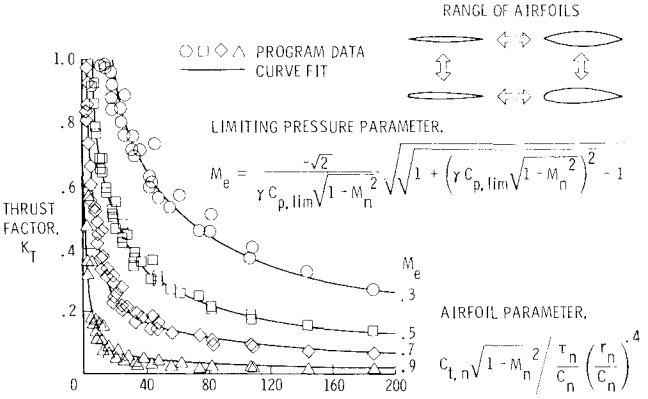


**Fig. 7 Thrust factor dependence on airfoil parameters for an arbitrary pressure limitation.**

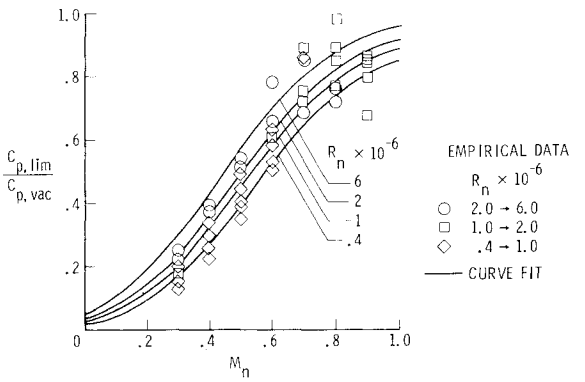


**Fig. 9 Limiting pressure coefficient dependence on normal Mach number and Reynolds number.**

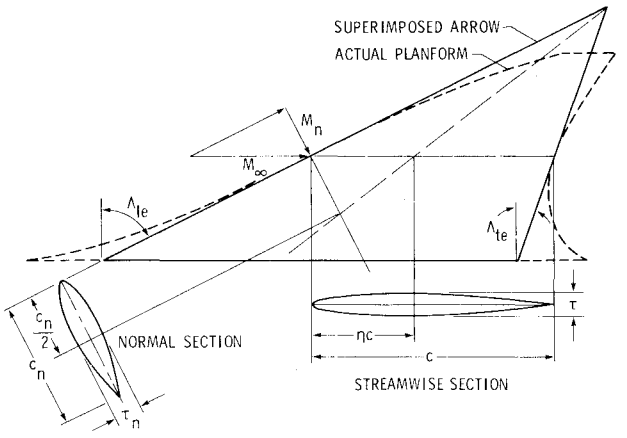


**Fig. 10 Definition of normal airfoil sections for three-dimensional wings.**

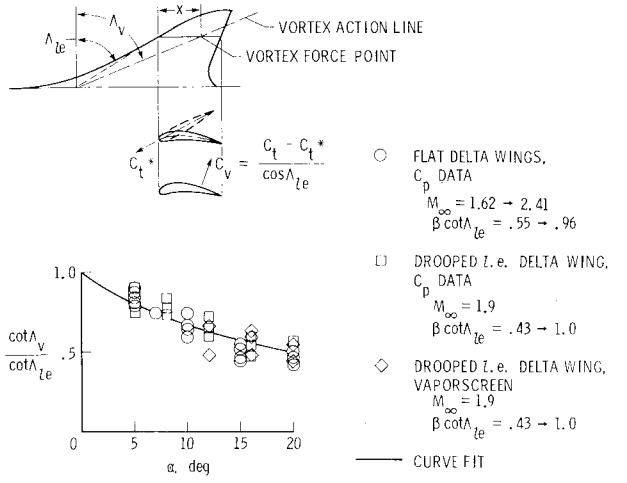


**Fig. 11 Estimation of vortex force location.**

assumed that, through the transformations discussed, the streamwise section leading-edge thrust characteristics can be related to the characteristics of a two-dimensional section which is normal to the leading edge and operates in a velocity field defined by the normal flow vector. To define the airfoil section normal to the leading edge at any given span station, a superimposed arrow wing is introduced. This phantom wing has the same sweep angles of the leading edge, the trailing edge, and the maximum-thickness line as does the actual wing at the same span station. Derivations of the following relationships between normal and streamwise quantities are given in the appendix of Ref. 4.

The normal flow Mach number is defined as

$$M_n = M_\infty \cos\Lambda_{le} \tag{5}$$

The chord of the normal section is defined in order to place the maximum thickness at midchord. The ratio of the normal section chord to the streamwise section chord may be expressed as

$$\frac{c_n}{c} = \frac{2\eta}{\sin\Lambda_{le}\left[(1-\eta)\tan\Lambda_{le} + \eta\tan\Lambda_{te}\right] + \cos\Lambda_{le}} \tag{6}$$

For an unswept trailing edge, Eq. (6) simplifies to

$$\frac{c_n}{c} = \frac{2\eta\cos\Lambda_{le}}{1-\eta\sin^2\Lambda_{le}}$$

and for unswept leading and trailing edges, or two-dimensional sections, the equation may be further reduced to

$$\frac{c_n}{c} = 2\eta$$

The thickness-to-chord ratio of the normal section may be expressed as

$$\frac{\tau_n}{c_n} = \frac{\tau}{c}\frac{1}{2\eta\cos\Lambda_{le}} \tag{7}$$

and the ratio of the leading-edge radius to chord for the normal section is

$$\frac{r_n}{c_n} = \frac{r}{c}\frac{1}{2\eta\cos^2\Lambda_{le}} \tag{8}$$

The normal section thrust coefficient is related to the streamwise section thrust coefficient by

$$c_{t,n} = c_t \frac{c}{c_n}\frac{1}{\cos^2\Lambda_{le}} \tag{9}$$

The normal flow Reynolds number is

$$R_n = R\frac{c_n}{\bar{c}}\cos\Lambda_{le} \tag{10}$$

In regions of the wing leading edge away from the apex and away from the wing-body juncture, the preceding expressions are believed to provide a reasonable basis for two-dimensional analysis of leading-edge thrust phenomena. In those regions where the analysis is most questionable, thrust values are generally small and errors in the attainable levels should have little impact on the overall performance of the wing.

With this development of the relationship between streamwise and normal airfoil section parameters, the set of equations for use in prediction of attainable thrust is complete. The prediction process may be summarized as:

1) Equations (5-10) are used to define normal airfoil parameters as a function of streamwise airfoil parameters for a series of spanwise wing stations.

2) Equation (4) defines the effective limiting pressure coefficient as a function of the local normal Mach number and Reynolds number.

3) Equation (2) provides an effective local Mach number for use in Eq. (3) to define the ratio of the attainable thrust to the theoretical leading-edge thrust.

## VI. Separated Leading-Edge Vortex Considerations

For sharp leading-edge wings, for which it may be assumed that no leading-edge thrust develops, Polhamus[8] established a relationship between the normal force induced by the separated vortex flow and the theoretical leading-edge thrust. According to the Polhamus suction analogy, the suction vector, $C_t/\cos\Lambda_{le}$, is assumed to rotate to a position normal to the wing surface where it affects the normal force rather than the chord force. In the present method, which treats a partially developed leading-edge thrust, it would seem logical to consider a partial development of the vortex force. The simplest approach would be to equate the vortex force to the undeveloped thrust

$$c_v = (c_t - c_t^*)/\cos\Lambda_{le}$$

This treatment differs from that given in Ref. 4, where a gradual rotation of the thrust vector was postulated. As will be seen later, the present scheme provides a simpler way of handling thrust and vortex forces for wings with twist and camber.

The suction analogy provides no information on the point of application of the vortex force vector. There is an implied assumption that it acts just behind the leading edge since no provision is made for a loss in vortex-induced normal force that might result when any portion of the vortex flowfield lies behind the wing trailing edge. Since the vortex flowfield can act at locations which under some conditions may be far removed from the leading edge, accurate estimates of the vortex-induced normal force, and more particularly the pitching moment, can be made only with some knowledge of the location of the vortex flowfield.

For the special case of wings designed for supersonic cruise and operating at supersonic speeds, it appears that a simple empirical relationship shown in Fig. 11 may be used to provide an approximate location for the vortex action line. This case is simplified because wings designed for supersonic cruise tend to approach delta planforms and because delta wings at supersonic speeds display a conical flowfield. Data for delta wings from Refs. 9 and 10 were used to define the location of the center of the vortex flowfield as a function of the angle of attack. The data provided no discernable evidence of trends with the other parameters, Mach number, and sweep angle. The curve fit shown on the figure is given by

$$\frac{\cot\Lambda_v}{\cot\Lambda_{le}} = \frac{1}{1+2.7\tan\alpha}$$

The present method for estimation of attainable leading-edge thrust has been developed for flat wings with symmetrical sections. However, the method is adaptable to wings with limited twist and camber when it is coupled with lifting-surface programs capable of providing accurate theoretical leading-edge thrust distributions. Figure 11 will help to illustrate this application. Since the airfoil profile in the immediate vicinity of the leading edge has a dominant influence on thrust characteristics, it should be possible to analyze the attainable thrust by performing calculations for a comparable symmetric wing section. This section would have a plane of symmetry which is tangent to the mean camber surface of the nonsymmetrical section at the leading edge. The superimposed symmetrical section could be assumed to have the same thickness ratio, leading-edge radius, and location of maximum thickness as the cambered section. The thrust vector would be assumed to act at an angle with respect to the wing-chord plane defined by the tangent to the camber surface. The vortex force would be assumed to act at a point defined by the vortex action line and to act normal to the wing surface. For a cambered wing, the vortex force can thus contribute to chord force as well as the normal force and the pitching moment.

For the examples given in this paper, the empirical vortex action line relationship was used to locate the vortex force at supersonic speeds only. With some diligent work, it might be possible to devise similar charts for certain classes of wings at subsonic speeds. In the absence of such information, the subsonic calculations were based on the assumption of a vortex force acting at the leading edge.

## VII. Comparisons with Experimental Data

Since the prediction method is based on two-dimensional flow considerations, it should work well for wings with little or no leading-edge sweep (an example is given in Ref. 4). A more severe test of the method will be given in correlations with data for wings with large leading-edge sweep angles, as shown in Figs. 12-15. Theoretical leading-edge thrust distributions were evaluated for subsonic and supersonic speeds by means of computer programs described in Refs. 1 and 4, respectively. The attainable thrust estimate was then obtained by input of these distributions into a special, separate computer program which implemented the computational process previously described. In computing the lift curve slope and the theoretical thrust distribution, the complete wing planform through the body was employed. This was done so that body carryover lift would not be neglected in the calculation of total lift and in the determination of leading-edge thrust. However, after theoretical leading-edge thrust distributions were obtained, that portion of the thrust inboard of the wing-body juncture was ignored. Theoretical lift and drag coefficients were formulated in order to be compatible with the Polhamus leading-edge suction analogy as described in Sec. VI.

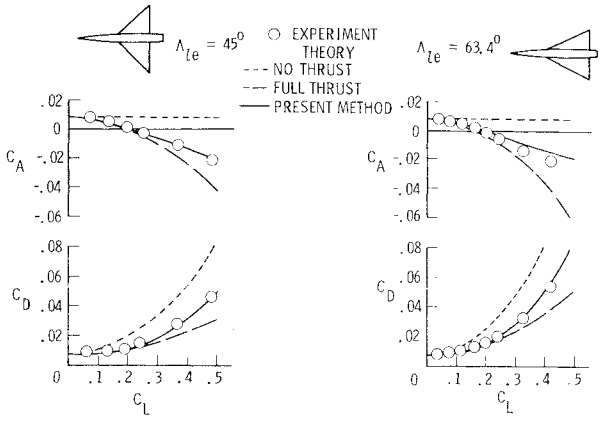


**Fig. 12 Comparison of theory and experiment for two leading-edge sweep angles.**

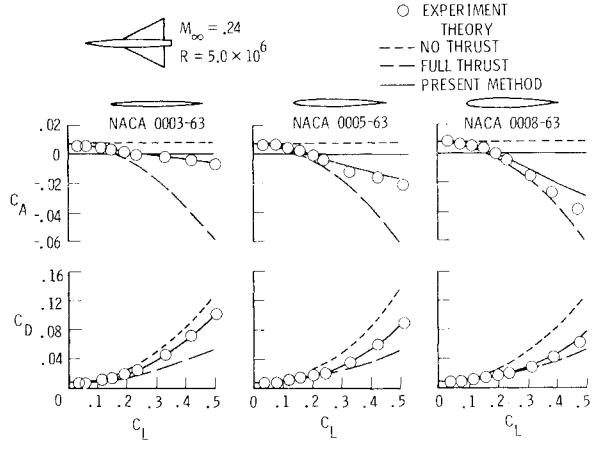


**Fig. 13 Comparison of theory and experiment for three thickness ratios.**

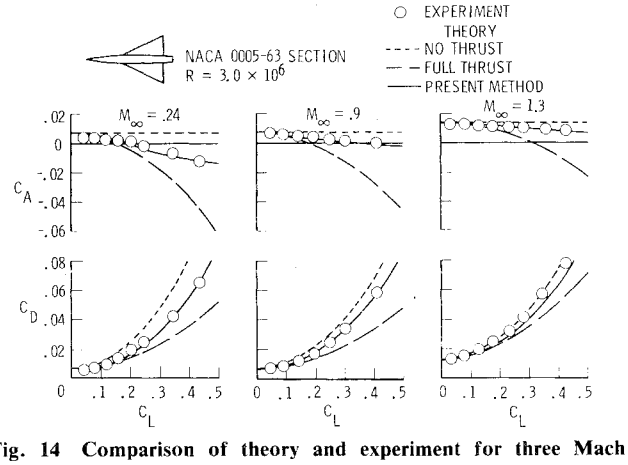


**Fig. 14 Comparison of theory and experiment for three Mach numbers.**

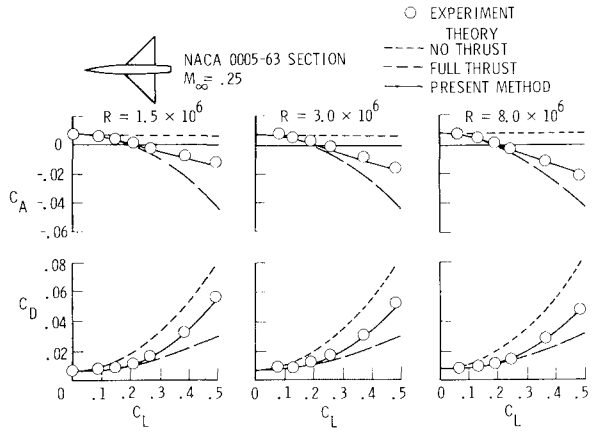


**Fig. 15 Comparison of theory and experiment for three Reynolds numbers.**

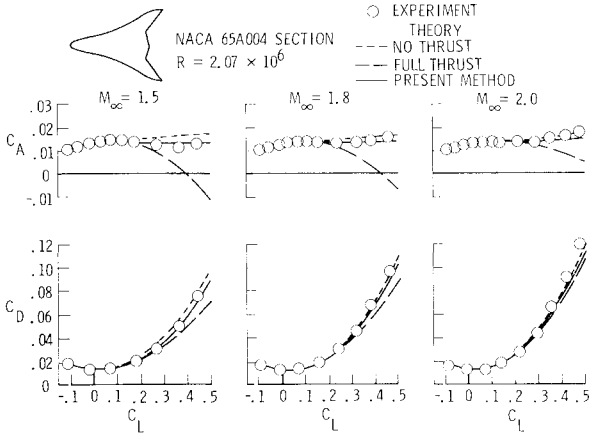


**Fig. 16 Comparison of theory and experiment for a twisted and cambered wing.**

The comparisons of theory and experiment shown in Figs. 12-16 are all of the same form. Axial force coefficient and drag coefficient are given as functions of the lift coefficient. The axial force is obviously the most sensitive indicator of the presence of leading-edge thrust and should be the primary gage of the success of failure of the estimation method. In observing the lift coefficient-drag coefficient polar, the transition from full or near-full thrust at low-lift coefficients to smaller values of thrust at high-lift coefficients is of interest. The lift curve slope, which is not shown here, is defined by the basic lifting surface program, and the degree of leading-edge thrust has only a small influence. For these correlations, no attempt was made to calculate theoretical zero-lift drag; instead, the experimental drag was used. To help assess the importance of leading-edge thrust, theoretical data are shown for the limiting conditions of zero and full theoretical thrust. In these figures, one parameter varies as the others remain essentially constant, to provide a test of trends predicted by the new method.

In Fig. 12, data are shown for delta wings with leading-edge sweep angles of 45.0 and 63.4 deg.[11] In both instances, the new method gives a good estimate of the measured aerodynamic characteristics at a Mach number of 0.25 for the 5%-thick wing. For the 63.4 deg swept wing, the prediction of lift and drag is seen to be reasonably good in spite of some error in the axial force.

The three parts of Fig. 13 show data for a 63.4 deg swept delta wing with thickness ratios of 3,5, and 8% at a Mach number of 0.24 and a Reynolds number of about $5 \times 10^6$.[11] Except for the 8%-thick wing, there is no appreciable discrepancy between the experimental data and the estimate by the present method. For this sweep angle and this wing section, the normal airfoil thickness ratio is about 0.3; whereas, the largest thickness ratio used in derivation of the thrust factors was 0.18. However, there is a reasonably good prediction of the lift-drag ratio in spite of the discrepancy between predicted and measured thrust at the higher lift coefficients.

The variation of attainable thrust with Mach number may be observed in the three parts of Fig. 14. The wing is a 63.4 deg swept delta with a 5%-thick section.[11] At a Mach number of 0.24, the data are little different from that seen previously. At a Mach number of 0.9, the experimental data and the prediction show a decrease in attainable thrust; but this does not result in a decrease in the lift-drag ratio because of the higher lift-curve slope. Because of the difficulty of predicting transonic flows, the good correlation shown here may be somewhat fortuitous. At the supersonic Mach number of 1.3, there is still evidence of some degree of leading-edge thrust. Although the thrust characteristics are well predicted, there is an appreciable difference in the lift-drag ratios. A discrepancy between the theoretical and measured lift at 0 deg angle of attack accounts for most of this difference.

The variation of attainable thrust with Reynolds number may be explored with the aid of data from Ref. 11 shown in Fig. 15. The range of Reynolds numbers covered is not as large as desired; nevertheless, Reynolds number trends are evident. Thrust levels and trends indicated by the predicted axial force coefficient agree closely with the experimental data.

Data at three supersonic speeds for a twisted and cambered wing with a complex planform shape[12] are shown in Fig. 16. It is seen that the present method provides a more accurate estimate of the variation of chord force with lift coefficient than does either the zero thrust or full-thrust theory. However, this does not necessarily produce a corresponding increase in accuracy of the variation of drag with lift. At these higher supersonic Mach numbers, the linearized theory estimate of the wing normal force is subject to errors because of nonlinearities in the real flow (for example, the influence of vacuum pressure limitations and the tendency for compression pressures to increase at a greater than linear rate with increasing local slope). These other sources of error must be taken into account in order to provide an increase in accuracy of the overall estimate of wing aerodynamic characteristics for supersonic speeds.

## VIII. Design Application

Because the present method of predicting attainable leading-edge thrust takes into account the spanwise variation of airfoil section characteristics, an opportunity is afforded for design by iteration to maximize the attainable thrust and the attendant performance benefits. The design may take into account variations in planform shape or spanwise variations of any of the wing section parameters. An example of design application of the prediction method is given in Ref. 4.

Application of the present method to the design of wings for supersonic cruise vehicles is of particular interest. Thrust considerations are normally ignored in supersonic aerodynamic theory, and wing lifting efficiency is optimized through use of twist and camber alone (e.g., Ref. 13). The resultant wing camber surfaces, however, may be too severe for incorporation into practical airplane designs. The large root chord angles and the resultant large cabin floor angles are particularly troublesome. If design by iteration using the present method could result in attainment of near-theoretical leading-edge thrust over even a limited range of angle of attack or lift coefficient, the wing design lift coefficient and the resultant camber surface severity could be reduced accordingly with little or no loss in aerodynamic efficiency. Some of the implications of thrust consideration in the design of vehicles for supersonic cruise are discussed in Ref. 14.

## IX. Concluding Remarks

A study of practical limitations on achievement of theoretical leading-edge thrust has been made and an empirical method for estimation of attainable thrust has been developed. The method is based on 1) a theoretical analysis of a set of two-dimensional airfoils to define thrust dependence on airfoil geometric characteristics and arbitrarily defined limiting pressures, 2) an examination of two-dimensional airfoil experimental data to provide an estimate of limiting pressure dependence on local Mach number and Reynolds number, and 3) employment of simple sweep theory to adapt the method to three-dimensional wings. Because the method takes into account the spanwise variation of airfoil section characteristics, an opportunity is afforded for design by iteration to maximize the attainable thrust and the attendant performance benefits. The applicability of the method was demonstrated by comparisons of theoretical and experimental aerodynamic characteristics for a series of wing-body configurations. Generally, good predictions of the attainable thrust and its influence on lift and drag characteristics were obtained over a range of Mach numbers from 0.24 to 2.0.

## References

[1] Lamar, J. E. and Gloss, B.B., "Subsonic Aerodynamic Characteristics of Interacting Lifting Surfaces With Separated Flow Around Sharp Edges Predicted by a Vortex-Lattice Method," NASA TN D-7921, 1975.

[2] Jones, R.T., "Estimated Lift-Drag Ratios at Supersonic Speed," NACA TN 1350, 1947.

[3] Carlson, H. W. and Mack, R.J., "Estimation of Leading-Edge Thrust for Supersonic Wings of Arbitrary Planform," NASA TP-1270, 1978.

[4] Carlson, H.W., Mack, R.J., and Barger R.L., "Estimation of Attainable Leading-Edge Thrust for Wings at Subsonic and Supersonic Speeds," NASA TP-1500, 1979.

[5] Bauer, F., Garabedian, P., Korn, D., and Jameson, A., "Supercritical Wing Sections II," *Lecture Notes in Economical and Mathematical Systems,* Vol. 108, Springer-Verlag, 1975.

[6] Daley, B. N. and Dick, R.S., "Effect of Thickness, Camber and Thickness Distribution on Airfoil Characteristics at Mach Numbers up to 1.0," NACA TN 3607, 1956 (supersedes NACA RM L52G31a).

[7] Loftin, L.K., Jr., "Aerodynamic Characteristics of the NACA 64-010 and 0010-1.10 40/1.051 Airfoil Sections at Mach Numbers From 0.30 to 0.85 and Reynolds Numbers From $4.0 \times 10^6$ to $8.0 \times 10^6$," NACA TN 3244, 1954.

[8] Polhamus, E.C., "Predictions of Vortex-Lift Characteristics by a Leading-Edge Suction Analogy," *Journal of Aircraft,* Vol. 8, April 1971, pp. 193-199.

[9] Boatright, W.B., "Experimental Study and Analysis of Leading and Pressure Distributions on Delta Wings Due to Thickness and to Angle of Attack at Supersonic Speeds," NACA RM L56I14, 1956.

[10] Michael, W.H., Jr., "Flow Studies on Drooped-Leading-Edge Delta Wings at Supersonic Speeds," NACA TN 3614, 1956.

[11] Hall, C.F., "Lift, Drag, and Pitching Moment of Low-Aspect-Ratio Wings at Subsonic and Supersonic Speeds," NACA TM A53A30, 1953.

[12] Robins, A.W., Lamb, M., and Miller, D.S., "Aerodynamic Characteristics at Mach Numbers of 1.5, 1.8, and 2.0 of a Blended Wing-Body Configuration With and Without Integral Canards," NASA TP-1427, 1979.

[13] Carlson, H.W. and Miller, D.S., "Numerical Methods for the Design and Analysis of Wings at Supersonic Speeds," NASA TN D-7713, 1974.

[14] Robins, A.W. and Carlson, H.W., "High-Performance Wings With Significant Leading-Edge Thrust at Supersonic Speeds," AIAA Paper 79-1871, New York, N.Y., Aug. 1979.